P2B.15 A TECHNIQUE FOR ANTICIPATING INITIAL RAPID INCREASES IN INTENSITY IN TROPICAL CYCLONES, USING 37 GHZ MICROWAVE IMAGERY

Margaret E. Kieper
Burnsville, MN

1. INTRODUCTION

An exhaustive review of available 37 gHz color pct microwave imagery for the 2003-2007 North Atlantic hurricane seasons yielded a relationship between patterns in the microwave imagery and periods of rapid intensification. This identified structural component was combined with the SHIPS Rapid Intensification Index, which primarily reflects environmental conditions, to produce a simple forecast methodology that was successful at hindcasting impending periods of rapid intensification in the best track.

2. IDENTIFYING PATTERNS IN THE 37 GHZ MICROWAVE IMAGERY

The 37 gHz color image uses a polarization correction (PCT) intended to distinguish between areas of deep convection and the sea surface, which can both have similar cold temperatures on microwave (MW) imagery, (Lee 2002), but which has the added benefit of easily distinguishing between shallow convective rainbands, which appear as cyan, and deep convection, which appears as pink. The 37 gHz color image primarily identifies precipitation, as evidenced by a comparison with a Doppler radar image from 2003 Claudette making landfall on the Texas coastline (Figure 1.). The images were nine minutes apart. The areas in pink on the MW correspond to a reflectivity of 35-55 dBZ on the radar image, and the light blue, to 20-35 dBZ; respectively, heavier and lighter precipitation. Details of the eye and moat areas (over water) are also similar.

Examination of 37 gHz color MW imagery reveals that the shallow rainband structure of the tropical cyclone (TC) is pivotal in the development of initial periods of rapid intensification (RI), defined as an increase of 30 kt or more in 24 hr (Kaplan and DeMaria 2003), that begin when the TC is at an initial intensity of at least 45 kt.

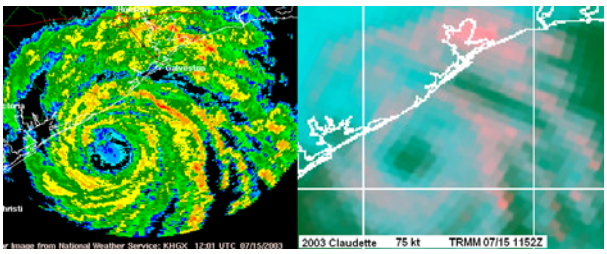

Figure 1. 2003 Hurricane Claudette, radar and MW

TC where RI occurred with an initial intensity less than 45 kt were rejected from the study because predicting an intensity increase of 30 kt to 60 kt, or 35 kt to 65 kt, was not an interesting forecast problem. TC that continued to intensify were picked up by the 45 kt threshold. This study also does not address subsequent periods of RI associated with eyewall replacement cycles (ERCs).

While a consistent initial pattern and subsequent trend in the pattern of deep convection also appear in all of the periods of RI in the study, it is the shallow convective precipitation in the core area of the TC that is initially present at the start of RI (more specifically, within plus or minus six hours of the beginning of RI, going by best track intensities), that appears to herald or reflect a fundamental shift in core dynamics related to RI. This symmetric accumulation of shallow precipitation around a precipitation-free center is identified as the **thick ring** pattern (Figure 2.), and appears either as a ring, in the case of a larger center, or nascent eye, or a **plate** structure (Figure 3.), with smaller eyes. In this sense the 37 gHz MW imagery provides a unique view of the TC structure that is not visible on the more-frequently-utilized 85 gHz that, while providing a higher resolution, mainly emphasizes deep convection.

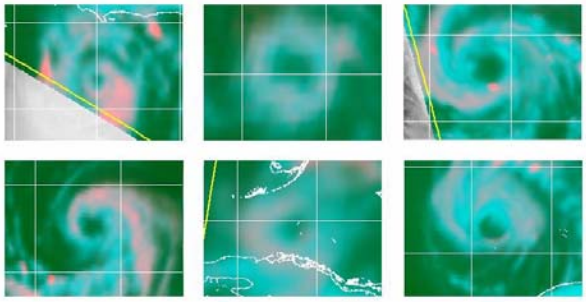

Figure 2. Examples of "thick ring" pattern (larger eyes); from L to R, top to bottom, 2005 Dennis, 2003 Isabel, 2006 Helene, 2004 Ivan, 2005 Rita, 2005 Emily (in the BOC)

And because 37 gHz is a lower resolution, identifying patterns in these MW images relies on the availability of images from newer sensors including TRMM, AMSR-E, and WindSat, although SSMI can be used for very large eyes, or to provide continuity between higher-resolution images. Only in recent years has there been a critical mass of available MW imagery at this higher resolution. In this study, a minimum of one image per six-hour forecast cycle was usually available to identify the onset of RI (and MW passes sometimes miss the center of the TC), but it is likely that more frequent MW imagery

would reveal additional details about the process of TC development.

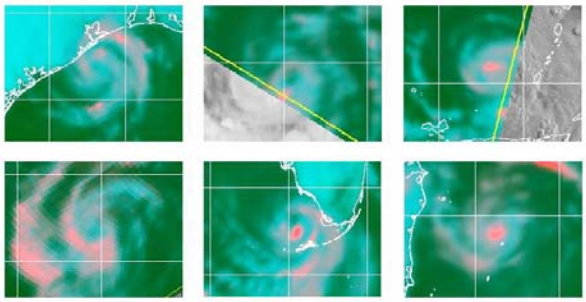

Figure 3. Examples of "plate ring" pattern (smaller eyes): 2007 Humberto, 2005 Wilma, 2005 Emily, 2004 Frances, 2005 Katrina, 2005 Beta

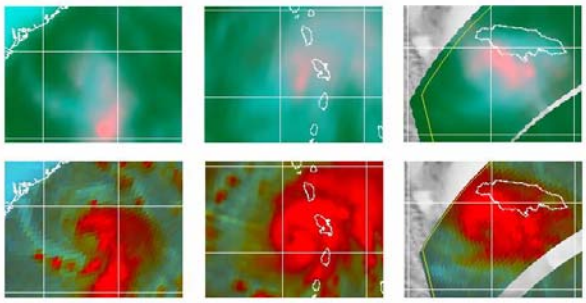

Figure 4. Plate ring pattern on lower-resolution SSMI MW imagery with corresponding 85 gHz image below the 37 gHz: 2004 Alex, 2007 Dean 2nd intensification, 2004 Charley

Using lower-resolution 37 gHz is very difficult unless the ring is large, as in the above examples of Isabel and Rita, but provided are three examples of plate rings in the SSMI imagery with partial banding deep convection along the outer edge (Figure 4). The 85 gHz color pct, below, confirms organized convection wrapping around the center.

3. TRENDS IN TC ORGANIZATION AND STRUCTURE

In order to ascertain whether the ring structure was unique to periods of intensification, the complete record of 37 gHz MW imagery was reviewed for all 82 TC in the five-year period. Other patterns in the MW imagery were identified in this process, in case they might have any significance. Over 5000 images were individually downloaded from the Naval Research Lab, Monterey tropical cyclone web site, reviewed, and catalogued.

The ring pattern did not occur in the majority of TC (48 out of 82). It occurred more than once in a handful of TC that strengthened, then weakened (sometimes due to land interaction, sometimes due to adverse environmental conditions), and began the strengthening process again: 2004 Alex, Jeanne and Lisa, 2005 Emily, Katrina, and Wilma, and 2007 Dean (yielding 41 cases resulting from 34 TC). Out of these 41 cases, seven were removed from the evaluation group because the ring pattern appeared just prior to landfall.

In the remaining 34 cases, the ring pattern consistently appeared at the beginning of all periods of RI (23 cases), but it also appeared in a smaller number of TC that did not go through RI (11 cases). There were no differences of note in the appearance of the ring pattern between the TC that went through RI, and those that did not (examples are shown in Figures 5. and 6.).

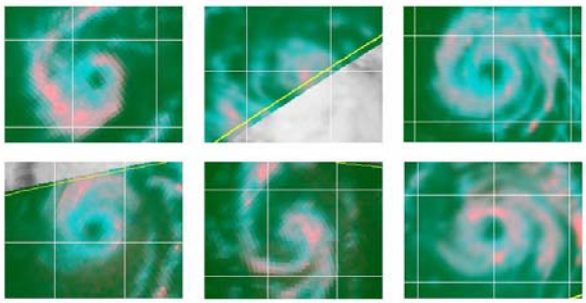

Figure 5. Comparison of initial "thick ring" pattern in TC that went through RI (top row: 2004 Danielle, 2004 Karl, 2006 Gordon) and those that did not (bottom row: 2004 Alex, at higher latitudes, 2003 Danny, 2005 Nate)

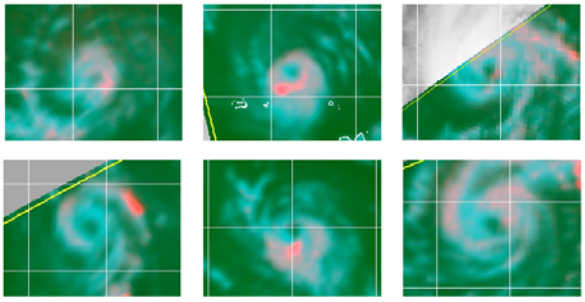

Figure 6. Comparison of initial "plate ring" pattern in TC that went through RI (top row: 2007 Dean, 1st intensification, 2007 Felix, 2003 Fabian) and those that did not (bottom row: 2005 Irene, 2004 Lisa, 2005 Ophelia)

Initially a method of differentiating between these two groups of TC was comparison of the changes in TC structure revealed in MW images over the subsequent 24-hour period. During a period of RI, successive MW images revealed patterns identifying a continually-improving trend in structural organization. Conversely, tropical cyclones that failed to maintain a trend of improved organization did not undergo rapid increases in intensity.

However these trends are not discernable until the period of RI is almost complete, and, coupled with the time delay in reception of MW imagery, which can be up to three hours on descending passes, are not timely with respect to the operational forecast cycle. But it was

found that different trends in organization correlated with a general range of intensity change.

3.1 TYPES OF TRENDS AND ASSOCIATED INTENSITY RANGES

All TC that went through RI had a **rapidly-improving trend in structural organization**. The characteristics of this trend are:

- on a larger scale beyond the core area, the shallow rainband structure changes dramatically during the course of the RI, reflecting a dynamic process
- thin bands of deep convection initially migrate (usually from a primary convective band) to the outer edge of the thick ring, and, then, over the course of the period of RI, to the center of the ring, and then to the inner edge of the ring
- the inner diameter of the shallow convective ring bordering the eye decreases over time
- the inner diameter of the shallow convective ring may begin as irregular but then transitions to symmetric and smooth
- the diameter of the deep convective band associated with the ring decreases over time
- the radial coverage of the deep convective band increases over time

A series of MW images from 2004 Ivan over a 36-hour period of RI (Figure 7.) demonstrates many of these characteristics.

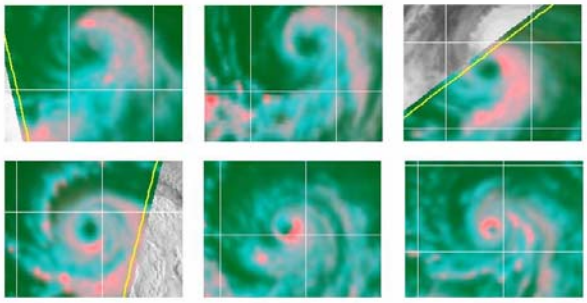

Figure 7. 2004 Hurricane Ivan, showing a rapid improving trend in organization, while increasing in intensity from 50 kt to 115 kt in a 36-hour period

TC that increased in the range of 15-20 kt in the 24-hour period following the appearance of the ring pattern had a **mixed trend in structural organization**. That is, there were some of the positive features identified with rapidly-improving trends, but there were also some indications of a declining trend in organization. These were generally the opposite of the positive features: for example, the inner radius of the shallow ring increased or stayed the same, rather than decreased. Two examples of this type of trend are 2003 Juan intensifying from 70 kt to 90 kt, and 2005 Irene intensifying from 45 kt to 60 kt (Figure 8.). Both TC begin with a similar thick plate ring, with banding deep convection along part of the outer edge. However, while Juan shows the pattern of deep convective banding decreasing in diameter around the center, the inner diameter of the shallow convective ring loses symmetry and never decreases. And Irene's shallow convective ring erodes, is regained, and erodes again, and no significant gains are made in the amount of deep convection.

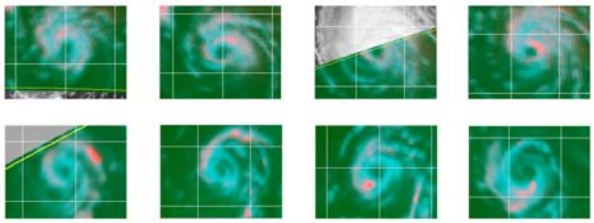

Figure 8. Mixed trend in organization, 2003 Juan (top) and 2005 Irene (bottom)

Interestingly, TC can still maintain or gain intensity over the short term even when the structural organization does not improve. An example of a **static trend with little change in organization** is shown in images of 2005 Epsilon over a 32-hour period, where intensity increased slightly, from 65 kt to 70 kt. But with a **rapidly-declining trend**, generally a TC will lose intensity quickly, as shown in a series of images of 2004 Lisa over a 24-hour period (Figure 9.), where intensity dropped from 60 kt to 50 kt.

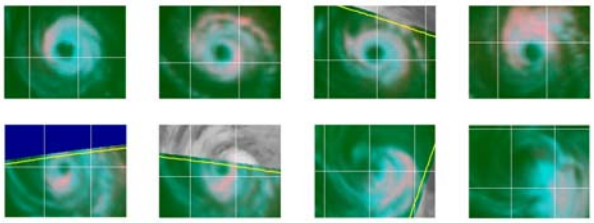

Figure 9. Little change in organization, 2005 Epsilon (top), rapid declining trend, 2004 Lisa (bottom)

4. DEVELOPING AND VERIFYING A FORECAST METHODOLOGY

While the success rate of identifying RI using the initial ring structure was better than chance, with a false alarm ratio (FAR) of 39% and a probability of detection (POD) of 81%, it was not good enough to use in forecasting RI. A better method was sought. Because it was apparent that environmental conditions were a factor in whether intensification would occur in the period following the initial development of the ring pattern, and because the SHIPS Rapid Intensification Index (RII) mainly factored in the synoptic conditions, it was determined that this might be a good companion (personal correspondence with John Knaff and James Franklin). Accordingly, after obtaining new SHIPS runs for the most recent (2007) version of SHIPS, RII data was extracted and loaded

into a relational database with the best track data, to produce an annotated best track.

When the SHIPS RII scaled and discriminant values were identified for the best track point closest to the time of the MW image where the ring pattern first occurred, in the subset of 34 TC, both SHIPS values were much higher for the group of TC that went through RI, and the SHIPS RII discriminant value (hereafter referred to as RII-d) was above an arbitrary threshold (>= 20%) for all of the TC that went through RI, and below the threshold for all but one of the others, yielding a hit ratio of 22/23, ten correct rejections, and one false alarm (Table 1).

However, a range of plus or minus six hours from the start of RI for the ring to form, while correctly reflecting the frequency of available MW imagery, was not suitable for an operational forecast methodology. At NHC, in order for a MW image to be utilized in a forecast, it has to be available by two hours into the start of the forecast cycle.

Readjusting the timing of the "arrival" of the MW image forward, in relation to the next available forecast cycle, resulted in four periods of RI being missed by six hours. The final statistics of the forecast methodology were 19 hits, four misses, and one false alarm, yielding a FAR of 5% (and corresponding success ratio, SR, of 95%), without changing the POD too much from what it had been prior to incorporating SHIPS: 83% (Table 2).

The final forecast methodology:

- **Once an intensifying TC reaches 45 kt, review subsequent 37 gHz MW for a thick ring pattern.**
- **If and when the ring pattern appears, if the SHIPS RII discriminant value for the forecast cycle where the pattern appears is >= 20%, forecast RI.**

5. OTHER MW PATTERNS OF NOTE

TC with subtropical characteristics have a distinctive and different appearance on the MW imagery, including a thin shallow convective ring but a broad area of heavy rainfall depicted by an overlay of pink, and a short tail (Figure 10.).

Many TC first develop a primary convective band, and the complete ring pattern is often first preceded by a partial shallow convective ring around the center, that is connected to the primary convective band by a bridging band of shallow convection (Figure 11.).

Once the complete ring pattern forms, deep convection often migrates from the primary convective band to the outer edge of the ring. In many cases as the core develops the primary convective band atrophies. However this early development is no guarantee of continued development. Of the three TC pictured, 2003 Nicholas never developed a complete ring, and 2003 Kate developed a thick ring pattern, but only gained 15 kt (both had SHIPS RII-d values below the threshold of 20% and so were not hindcast to go through RI).

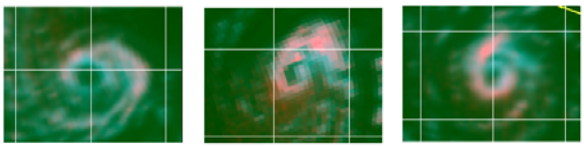

Figure 10. TC with subtropical characteristics: 2005 Epsilon, 2003 Ana, 2005 Vince

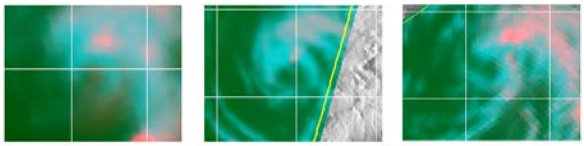

Figure 11. TC with a partial shallow convective ring attached to the primary convective band: 2003 Kate, 2006 Gordon, 2003 Nicholas

6. FUTURE WORK

The consistency of the timing of the thick ring pattern with respect to periods of rapid intensification leads to anticipation of tying the MW imagery to published theory on TC dynamics (Chris Rozoff, CIMSS, personal correspondence).

Evaluation of recon data around the timing of the development of the thick ring pattern may lead to specifics that can help identify the beginning of potential periods of RI from recon data, relating to 37 gHz MW patterns, and also possibly a link to when the wind gradient field begins to tighten (Jack Beven, NHC, personal correspondence).

Automation of the ring detection from MW data and incorporation into automated intensity forecast products (John Knaff, CIRA and Chris Rozoff, CIMSS, personal correspondence).

7. ACKNOWLEDGMENTS

Radar image courtesy of NWS SRH; all other images courtesy of Naval Research Lab, Monterey

SHIPS RII rerun for 2003-2007 courtesy of John Kaplan and John Knaff

8. REFERENCES

Kaplan, J, DeMaria, M (2003) "Large-scale characteristics of rapidly intensifying tropical cyclones in the north Atlantic basin" Wea Forecast 18: 1093-1108

Lee (2002) NRL TRMM 37 gHz Color Tutorial, http://www.nrlmry.navy.mil/sat_training/tropical_cyclones/trmm/37pct/index.html

Table 1. The best track times used for the hindcast for TC having the MW ring pattern, and the values of the SHIPS Rapid Intensification Index for the time the pattern occurred. Successfully-forecast periods of RI are highlighted with the SHIPS RII-d value above the threshold of 20% in green, and the intensity increase during the period of RI highlighted in aqua. The false alarm is highlighted in pink. Correct rejections with the SHIPS RII-d value below 20% are highlighted in orange.

named storm	RII-s %	RII-d %	inten-sity change	best track starting time	best track ending time	time of MW pass with ring pattern	delta from start of forecast cycle (hr)
2005 Wilma	40	43	90 kt	60 kt 10/18 0600Z	150 kt 10/19 0600Z	10/18 0206Z TRMM	-4.0
2007 Felix	35	46	85 kt	65 kt 09/02 0000Z	150 kt 09/03 0000Z	09/01 2148Z WindSat	-2.0
2004 Ivan	38	41	55 kt	60 kt 09/05 0000Z	115 kt 09/06 0000Z	09/04 2043Z WindSat	-3.0
2005 Rita	34	32	60 kt	85 kt 09/20 1800Z	145 kt 09/21 1800Z	09/20 1323Z SSMIS	-4.5
2003 Isabel	35	34	45 kt	65 kt 09/07 1200Z	110 kt 09/08 1200Z	09/07 0906Z SSMI	-3.0
2003 Fabian	36	34	40 kt	70 kt 08/30 0600Z	110 kt 08/31 0600Z	08/30 0217Z TRMM	-3.5
2005 Dennis	48	45	40 kt	90 kt 07/07 1200Z	130 kt 07/08 1200Z	07/07 0542Z TRMM	-6.0
2006 Gordon	36	35	25 kt	80 kt 09/13 1200Z	105 kt 09/14 1200Z	09/13 1005Z WindSat	-2.0
2007 Dean (1)	15	22	30 kt	50 kt 08/15 1200Z	80 kt 08/16 1200Z	08/15 1322Z TRMM	1.5
2006 Helene	27	22	30 kt	70 kt 09/17 0000Z	100 kt 09/18 0000Z	09/16 2026Z WindSat	-3.5
2005 Katrina (leaving FL)	13	20	30 kt	65 kt 08/26 0600Z	95 kt 08/27 0600Z	08/26 0339Z TRMM	-2.5
2004 Alex (1)	28	27	35 kt	50 kt 08/02 1800Z	85 kt 08/03 1800Z	08/02 1312Z SSMI	-5.0
2004 Danielle	17	27	30 kt	55 kt 08/14 18000Z	85 kt 08/15 1800Z	08/14 1527Z TRMM	-2.5
2004 Frances	43	45	35 kt	55 kt 08/26 1200Z	90 kt 08/27 1200Z	08/26 1049Z TRMM	-1.0
2005 Emily (1)	47	49	30 kt	85 kt 07/14 1200Z	115 kt 07/15 1200Z	07/14 1037Z WindSat	-1.5
2005 Emily (2)	31	28	30 kt	80 kt 07/19 0600Z	110 kt 07/20 0600Z	07/18 2359Z WindSat	-6.0
2004 Jeanne (2)	26	31	25 kt	50 kt 09/20 0000Z	75 kt 09/21 0000Z	09/19 1824Z AMSR-E	-5.5
2006 Florence	42	42	20 kt	60 kt 09/10 0000Z	80 kt 09/20 0000Z	09/09 2001Z TRMM	-4.0
2004 Karl	44	44	25 kt	7- kt 09/18 0000Z	95 kt 09/19 0000Z	09/17 2317Z TRMM	-0.5
2004 Charley (before Cuba)	29	35	30 kt	75 kt 08/12 0600Z	105 kt 08/13 0600Z	08/11 2359Z SSMI	-6.0
2007 Dean (2)	41	40	55 kt	90 kt 08/17 1200Z	145 kt 08/18 1200Z	08/17 1220Z SSMIS	0.5
2007 Humberto	13	27	25 kt *	55 kt 09/13 0000Z	80 kt 09/13 0600Z	09/12 2005Z AMSR-E	-4.0
2005 Beta	45	41	25 kt **	75 kt 10/29 1800Z	100 kt 10/30 0600Z	10/29 1140Z TRMM	-6.5
2005 Maria	35	23	25 kt	75 kt 09/05 0000Z	100 kt 09/06 0000Z	09/04 2007Z TRMM	-4.0
2004 Alex (2)	10	3	25 kt	80 kt 08/04 0600Z	105 kt 08/05 0600Z	08/04 0316Z TRMM	-3.0
2005 Irene	9	15	15 kt	45 kt 08/12 0000Z	60 kt 08/13 0000Z	08/11 2201Z WindSat	-2.0
2003 Kate	11	13	20 kt	55 kt 10/01 1200Z	75 kt 10/02 1200Z	10/01 1344Z TRMM	2.0
2003 Juan	7	6	20 kt	70 kt 09/26 1800Z	90 kt 09/27 1800Z	09/26 1816Z TRMM	0.0
2005 Nate	9	11	5 kt	70 kt 09/07 1800Z	75 kt 09/08 1800Z	09/07 1540Z TRMM	-2.5
2005 Ophelia	10	13	-5 kt	70 kt 09/10 1800Z	65 kt 09/11 1800Z	09/10 1428Z TRMM	-3.5
2005 Epsilon	4	3	0 kt	65 kt 12/02 1800Z	65 kt 12/03 1800Z	12/02 1942Z TRMM	2.0
2003 Danny	8	3	10 kt	55 kt 07/18 0600Z	65 kt 08/18 0600Z	07/18 0558Z TRMM	0.0
2004 Lisa (2)	10	5	-5 kt	60 kt 10/01 1800Z	55 kt 10/02 1800Z	10/01 2008Z TRMM	2.0
2004 Lisa (1)	9	13	-10 kt	60 kt 09/21 0600Z	50 kt 09/22 0600Z	09/21 0401Z AMSR-E	-2.0

* Humberto gained 25 kt in six hours
** Beta gained 25 kt in twelve hours

Table 2. TC having the initial thick ring pattern in the MW imagery, in relation to best track intensities and RI. The time of the initial MW ring pattern is in purple text. Successfully-forecast periods of RI are highlighted in light green, and misses in aqua. The false alarm is highlighted in pink.

2003 Fabian	50	60	65	70	85	100	110	110
2003 Isabel	55	60	65	70	80	95	110	110
2004 Alex	35	40	50	50	60	70	85	85
2004 Charley	65	65	75	80	90	90	105	95
2004 Danielle	35	40	45	55	65	75	80	85
2004 Frances	40	45	55	65	70	75	90	100
2004 Ivan	50	55	60	65	85	110	115	110
2004 Jeanne	40	40	45	50	55	60	75	75
2004 Karl	50	55	55	70	85	90	95	95
2005 Dennis	60	70	80	90	100	120	110	130
2005 Emily (1)	55	70	75	85	100	110	115	115
2005 Emily (2)	65	65	75	80	80	85	110	110
2005 Katrina	60	70	65	75	85	90	95	100
2005 Maria	65	65	75	75	80	85	90	100
2005 Rita	60	60	70	85	95	110	120	145
2005 Wilma	40	45	55	60	65	75	130	150
2005 Beta	60	70	75	75	80	100		
2006 Florence	50	50	50	60	70	75	80	80
2006 Gordon	55	65	70	80	95	105	105	105
2006 Helene	65	65	70	75	80	90	100	105
2007 Dean (1)	50	50	50	55	60	70	80	80
2007 Dean (2)	80	80	90	110	125	145	145	130
2007 Felix	40	50	60	65	85	90	115	150
2007 Humberto	25	35	45	55	80			